AMERICAN SOCIETY FOR MICROBIOLOGY | Antimicrobial Agents and Chemotherapy®

PHARMACOLOGY

Aerosolized Polymyxin B for Treatment of Respiratory Tract Infections: Determination of Pharmacokinetic-Pharmacodynamic Indices for Aerosolized Polymyxin B against *Pseudomonas aeruginosa* in a Mouse Lung Infection Model

Yu-Wei Lin,[a] Qi Zhou,[b] Nikolas J. Onufrak,[c] Veronika Wirth,[d] Ke Chen,[d] Jiping Wang,[d] Alan Forrest,[c] Hak-Kim Chan,[a] Jian Li[e]

Advanced Drug Delivery Group, Faculty of Pharmacy, The University of Sydney, Sydney, New South Wales, Australia[a]; Department of Industrial and Physical Pharmacy, College of Pharmacy, Purdue University, West Lafayette, Indiana, USA[b]; Department of Pharmacotherapy and Experimental Therapeutics, Eshelman School of Pharmacy, The University of North Carolina, Chapel Hill, North Carolina USA[c]; Drug Delivery, Disposition and Dynamics, Monash Institute of Pharmaceutical Sciences, Monash University (Parkville Campus), Parkville, Victoria, Australia[d]; Biomedicine Discovery Institute, Department of Microbiology, Monash University, Clayton, Victoria, Australia[e]

ABSTRACT Pulmonary administration of polymyxins is increasingly used for the treatment of respiratory tract infections caused by multidrug-resistant Gram-negative bacteria, such as those in patients with cystic fibrosis. However, there is a lack of pharmacokinetics (PK), pharmacodynamics (PD), and toxicity data of aerosolized polymyxin B to inform rational dosage selection. The PK and PD of polymyxin B following pulmonary and intravenous dosing were examined in neutropenic infected mice, and the data were analyzed by a population PK model. Dose fractionation study was performed for total daily doses between 2.06 and 24.8 mg base/kg of weight against *Pseudomonas aeruginosa* ATCC 27853, PAO1, and FADDI-PA022 (MIC of 1 mg/liter for all three strains). Histopathological examination of the lung was undertaken at 24 h posttreatment in both healthy and neutropenic infected mice. A two-compartment PK model was required for both epithelial lining fluid (ELF) and plasma drug exposure. The model consisted of central and peripheral compartments and was described by bidirectional first-order distribution clearance. The ratio of the area under the curve to the MIC (AUC/MIC) was the most predictive PK/PD index to describe the antimicrobial efficacy of aerosolized polymyxin B in treating lung infections in mice (R^2 of 0.70 to 0.88 for ELF and 0.70 to 0.87 for plasma). The AUC/MIC targets associated with bacteriostasis against the three *P. aeruginosa* strains were 1,326 to 1,506 in ELF and 3.14 to 4.03 in plasma. Histopathological results showed that polymyxin B aerosols significantly reduced lung inflammation and preserved lung epithelial integrity. This study highlights the advantageous PK/PD characteristics of pulmonary delivery of polymyxin B over intravenous administration in achieving high drug exposure in ELF.

KEYWORDS polymyxins, respiratory tract infections, pulmonary administration, *Pseudomonas aeruginosa*, antibiotic resistance, Gram-negative bacteria

The emergence of multidrug-resistant (MDR) Gram-negative bacteria, such as *Pseudomonas aeruginosa*, represents a major public health threat globally (1). Polymyxins are considered the last-line therapeutic option for these MDR Gram-negative

Received 3 February 2017 **Returned for modification** 2 April 2017 **Accepted** 20 May 2017

Accepted manuscript posted online 30 May 2017

Citation Lin Y-W, Zhou Q, Onufrak NJ, Wirth V, Chen K, Wang J, Forrest A, Chan H-K, Li J. 2017. Aerosolized polymyxin B for treatment of respiratory tract infections: determination of pharmacokinetic-pharmacodynamic indices for aerosolized polymyxin B against *Pseudomonas aeruginosa* in a mouse lung infection model. Antimicrob Agents Chemother 61:e00211-17. https://doi.org/10.1128/AAC.00211-17.

Copyright © 2017 American Society for Microbiology. All Rights Reserved.

Address correspondence to Hak-Kim Chan, kim.chan@sydney.edu.au, or Jian Li, jian.li@monash.edu.

pathogens (2, 3). Polymyxins are a class of multicomponent, polypeptide antibiotics, and there are two polymyxins available in the clinic, polymyxin B and colistin (i.e., polymyxin E), which differ by only an amino acid (4). Both polymyxins display similar *in vitro* pharmacodynamic (PD) properties (4). However, in clinical practice colistin is administered in the form of an inactive prodrug, colistin methanesulfonate (CMS), which subsequently converts to colistin *in vivo* (5), while polymyxin B is parenterally administered in its pharmacologically active sulfate salt form (6). They substantially differ in their plasma pharmacokinetic (PK) properties following intravenous administration in critically ill patients (2, 7–11). In patients with cystic fibrosis, the maximum plasma concentration ($C_{max,\ Plasma}$) of formed colistin following parenteral CMS (150 mg colistin base activity) ranged from 0.40 to 0.77 mg/liter (12). Even when a CMS loading dose is utilized, optimal plasma concentrations of formed colistin cannot be rapidly achieved (9, 13). Conversely, intravenous infusion of polymyxin B allows rapid attainment of relatively higher plasma concentrations (2.38 to 13.9 mg/liter) (13, 14). Although PK of polymyxin B in plasma following intravenous administration has been examined previously, very limited PK data are available for polymyxin B in epithelial lining fluid (ELF) following pulmonary or intravenous administration.

To date, the clinical use of polymyxins has been focused on parenteral administration (3, 15, 16). Only recently has the importance of aerosolized polymyxins for the treatment of respiratory tract infections started attracting significant interest (17–24). The majority of current preclinical and clinical PK/PD data for aerosolized polymyxins focus on CMS/colistin (12, 19, 21, 22, 25–27), although aerosolized polymyxin B has also been used in the clinic (28). There is currently a lack of reliable PK data of aerosolized polymyxin B to guide the dosage selection of inhalational therapy. As the systemic PK differ between the two polymyxins, it is important to examine the PK/PD of polymyxin B after pulmonary administration to maximize its efficacy while minimizing toxicity and development of resistance. Our study aimed to investigate the PK of aerosolized polymyxin B in a neutropenic mouse lung infection model. The population PK model enabled a better and quantitative understanding of polymyxin B disposition in ELF and plasma following both pulmonary and intravenous administration. Furthermore, this study aimed to identify the most predictive PK/PD index of polymyxin B that describes its efficacy against *P. aeruginosa* and to determine the magnitudes of the PK/PD index associated with different killing effects. Finally, the safety of aerosolized polymyxin B was assessed by histopathological examination of lung tissues.

RESULTS

PK of polymyxin B following intravenous and pulmonary administration. Figure 1 shows the concentration-time profiles of polymyxin B following intravenous administration of 4.12 mg base/kg of body weight polymyxin B and pulmonary administration of 4.12 and 8.24 mg base/kg polymyxin B. An average unbound fraction of 0.046 (unpublished data; methods are provided in the supplemental material) was used to generate the corresponding unbound polymyxin B concentration-time profiles (Fig. 1B). Intravenous administration of polymyxin B resulted in an average free plasma concentration of 1.07 $\pm$ 0.14 mg/liter at 5 min after administration and declined rapidly (Fig. 1). Following pulmonary administration of 4.12 or 8.24 mg base/kg polymyxin B, the maximum ELF concentration ($C_{max,\ ELF}$) was 107.0 $\pm$ 24.6 mg/liter or 184.0 $\pm$ 35.1 mg/liter, and the concentration was quantifiable over the 12-h sampling time (Fig. 1A and Table 1). After inhalation, polymyxin B was rapidly absorbed into the systemic circulation with a time to peak plasma concentration (T_{max}) of 15 min and $fC_{max,\ Plasma}$ of 0.46 $\pm$ 0.04 mg/liter (for 4.12 mg base/kg), which was significantly lower than the concentration at 15 min (0.84 $\pm$ 0.14 mg/liter) after intravenous administration (Fig. 1B and Table 1). The ELF concentration was below the ELF limit of quantification (LOQ) (i.e., ~2.00 mg/liter) following intravenous administration of 4.12 mg base/kg polymyxin B.

The PK profile of polymyxin B in both ELF and plasma following intravenous and pulmonary administration was well predicted by the developed population PK model (Fig. 2 and 3). A total of six data points were identified as outliers and excluded from

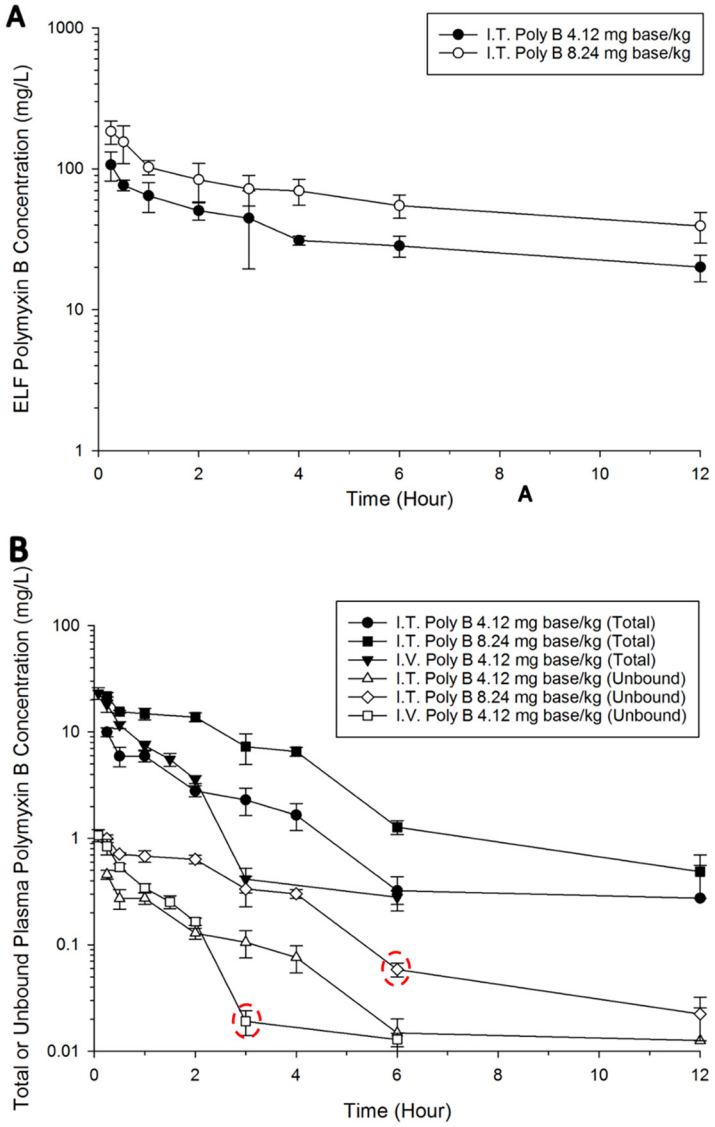

FIG 1 (A) Polymyxin B ELF concentration-time profiles following pulmonary (i.e., intratracheal [I.T.]) administration of 4.12 and 8.24 mg base/kg polymyxin B. The polymyxin B ELF concentration following intravenous (I.V.) administration was below the LOQ. (B) Total and unbound plasma polymyxin B concentration-time profiles after pulmonary (4.12 and 8.24 mg base/kg) and intravenous (4.12 mg base/kg) administration of polymyxin B in neutropenic lung-infected mice. Each symbol represents the means ± standard deviations (SD) (n = 3 or more). Six data points were excluded from the final population PK model. Data enclosed in circles were identified as potential outliers.

the final PK analysis (refer to Fig. 1 for the outliers). Overall, a two-compartment model was required to describe polymyxin B PK in both ELF and plasma following pulmonary and intravenous administrations (Fig. 4). The PK model estimated parameters are presented in Table 2. The model consisted of a central plasma compartment connected to a peripheral plasma compartment, with bidirectional transfer via first-order distribution clearance term ($CL_{D,\ Plasma}$). The rate of polymyxin B transfer from the ELF1 compartment to the central plasma compartment was bidirectional and described by two first-order clearance terms, $CL_{Plasma,\ ELF}$ (1.14×10^{-4} liters/h/kg; standard error [SE] of 4.69%) and $CL_{ELF,\ Plasma}$ (4.08×10^{-3} liters/h/kg; SE of 6.18%). Only the unbound fraction was assumed to be shared between central and peripheral plasma compartments, and the unbound fraction in plasma was fixed to 0.046. The low rate of transfer ($CL_{Plasma,\ ELF}$ of 1.14×10^{-4} liters/h/kg) from the central plasma compartment to the ELF1 compartment was adequate to explain the negligible ELF exposure after intrave-

TABLE 1 PK parameters for polymyxin B following pulmonary and intravenous administration in neutropenic infected mice

Parameter and sample source	Value after single dose		
	Pulmonary		Intravenous[a]
	4.12 mg base/kg	8.24 mg base/kg	4.12 mg base/kg
ELF			
$C_{max,\ ELF}$ (mg/liter)	107 ± 24.6	184 ± 35.1	NA
AUC_{ELF} (mg · h/liter)	601	1,203	<LOQ
Plasma			
$fC_{max,\ Plasma}$ (mg/liter)	0.46 ± 0.04	1.00 ± 0.08	NA
T_{max} (min)	15	15	NA
$fAUC_{Plasma}$ (mg · h/liter)	1.10	2.25	1.10

[a]NA, not applicable.

nous administration. Elimination from the biological system is described by a linear first-order total clearance (CL_{Total} of 3.54 liters/h/kg; SE of 0.48%) and originates only from the central plasma compartment. The estimated bioavailability after pulmonary administration was 99.3% (SE of 6.89%) (Table 2).

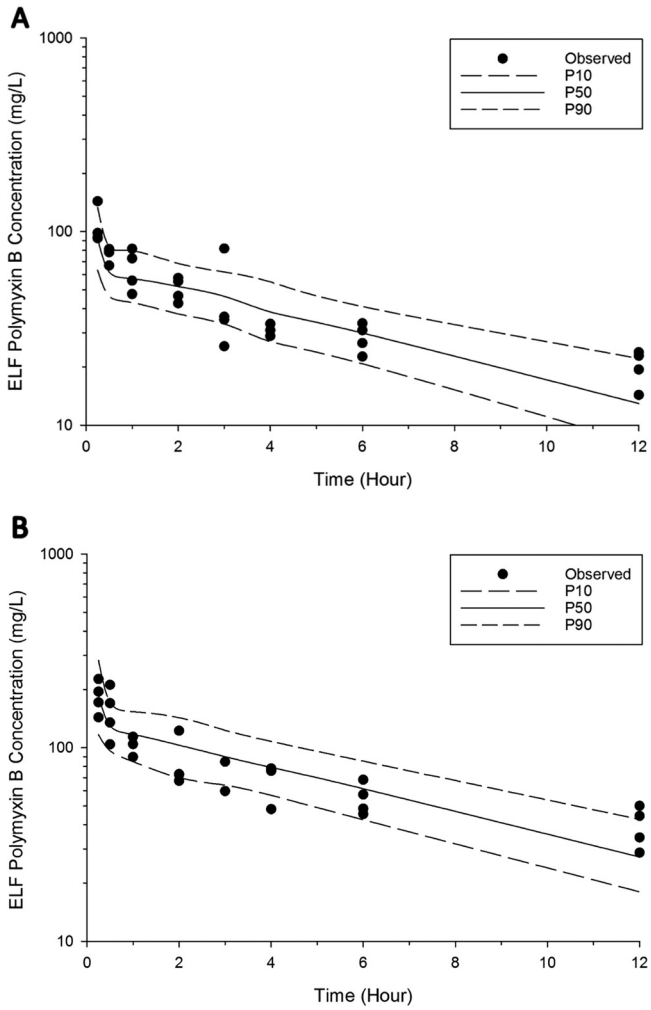

FIG 2 Visual predictive checks for polymyxin B in ELF following pulmonary administration of 4.12 mg base/kg (A) and 8.24 mg base/kg (B). The solid line represents the median model-predicted concentrations (P50); the broken lines represent the model-predicted 10th (P10) and 90th (P90) percentiles. The solid dots represent the observed concentrations.

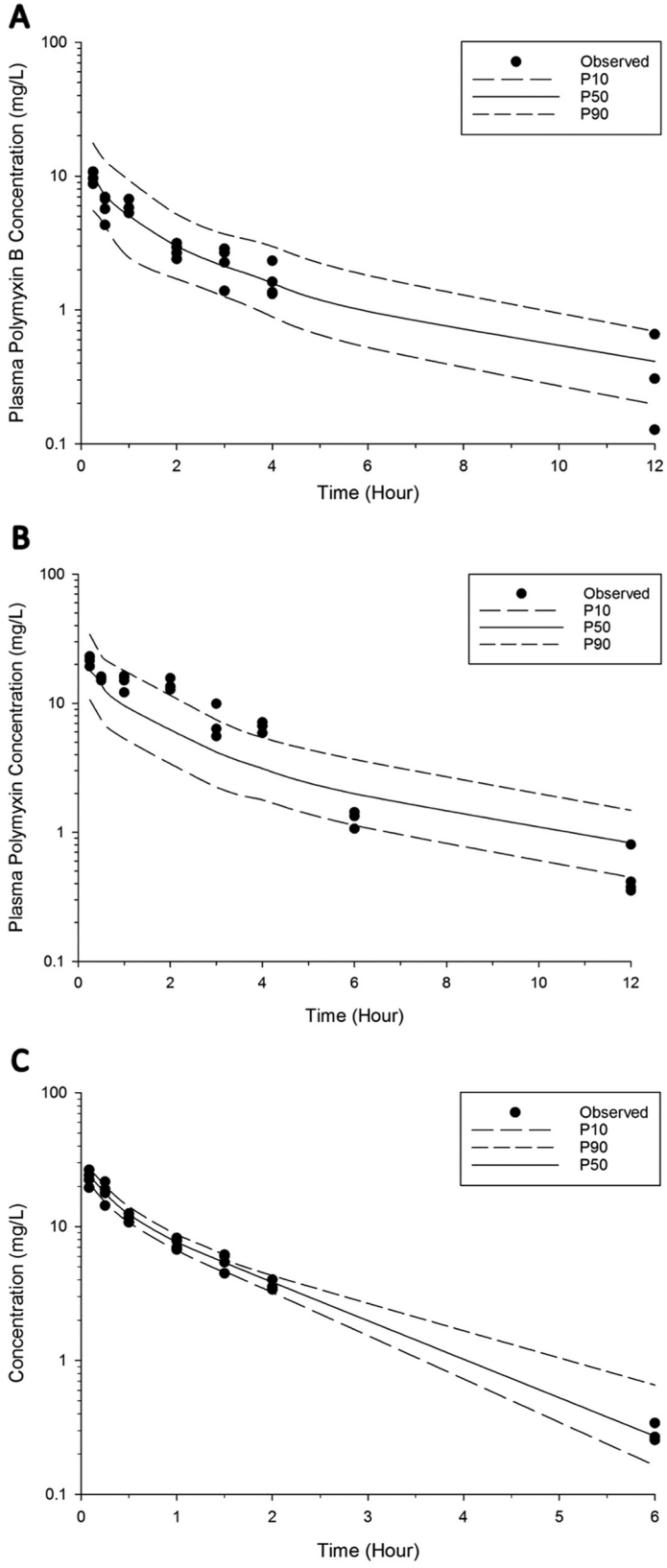

FIG 3 Visual predictive checks for polymyxin B in plasma following pulmonary administration of 4.12 mg base/kg (A) and 8.24 mg base/kg (B) and intravenous administration of 4.12 mg base/kg (C). The solid line represents the median model-predicted concentrations (P50); the broken lines represent the model predicted 10th (P10) and 90th (P90) percentiles. The solid dots represent the observed concentrations. Six data points were excluded from the final population PK model.

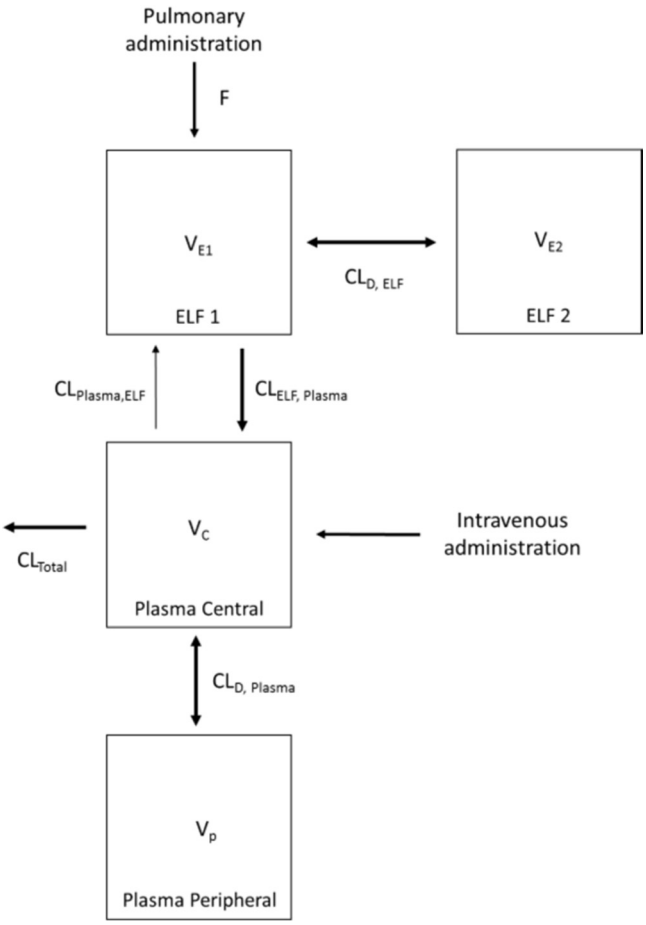

FIG 4 Schematic representation of the population PK model describing the disposition of polymyxin B following intravenous and pulmonary administration in neutropenic lung-infected mice.

PK/PD of aerosolized polymyxin B. The relationship between the ratio of the area under the curve to the MIC (AUC/MIC) and the ratio of C_{max} to MIC (C_{max}/MIC) in ELF or plasma and the bacterial load at 24 h is presented in Fig. 5. Based on the R^2 value and the dispersion of the observed data around the fitted function, AUC/MIC in ELF (AUC_{ELF}/MIC) and *f*AUC/MIC in plasma ($fAUC_{Plasma}$/MIC) was the most predictive of antimicrobial efficacy for all three tested *P. aeruginosa* strains (Table 3). The values of AUC/MIC associated with bacteriostasis and 1-log_{10} and 2-log_{10} kills are presented in

TABLE 2 Population PK parameter estimates for unbound polymyxin B after pulmonary and intravenous administration in neutropenic infected mice

Parameter	Description	Unit	Estimated value	SE[a] (%)
V_{E1}	ELF1 vol of distribution	Liters/kg	3.32×10^{-4}	11.7
V_{E2}	ELF2 vol of distribution	Liters/kg	1.49×10^{-2}	14.5
V_C	Vol of distribution of central plasma compartment	Liters/kg	3.06	2.05
V_P	Vol of distribution of peripheral plasma compartment	Liters/kg	1.56	1.15
$CL_{D, ELF}$	ELF intercompartmental clearance	Liters/h/kg	3.97×10^{-3}	2.07
$CL_{D, Plasma}$	Plasma intercompartmental clearance	Liters/h/kg	3.51	6.62
CL_{Total}	Total clearance	Liters/h/kg	3.54	0.48
$CL_{ELF, Plasma}$	Intercompartmental clearance ELF to plasma	Liters/h/kg	4.08×10^{-3}	6.18
$CL_{Plasma, ELF}$	Intercompartmental clearance plasma to ELF	Liters/h/kg	1.14×10^{-4}	4.69
f_u	Unbound fraction	%	4.60×10^{-2} (fixed)	NA
F	Bioavailability	%	99.3	6.89
$t_{1/2}$	Elimination half-life[b]	h	0.60	ND

[a]NA, not applicable; ND, not determined.
[b]Calculated using $t_{1/2} = \ln(2) \cdot V_C/CL_{Total}$.

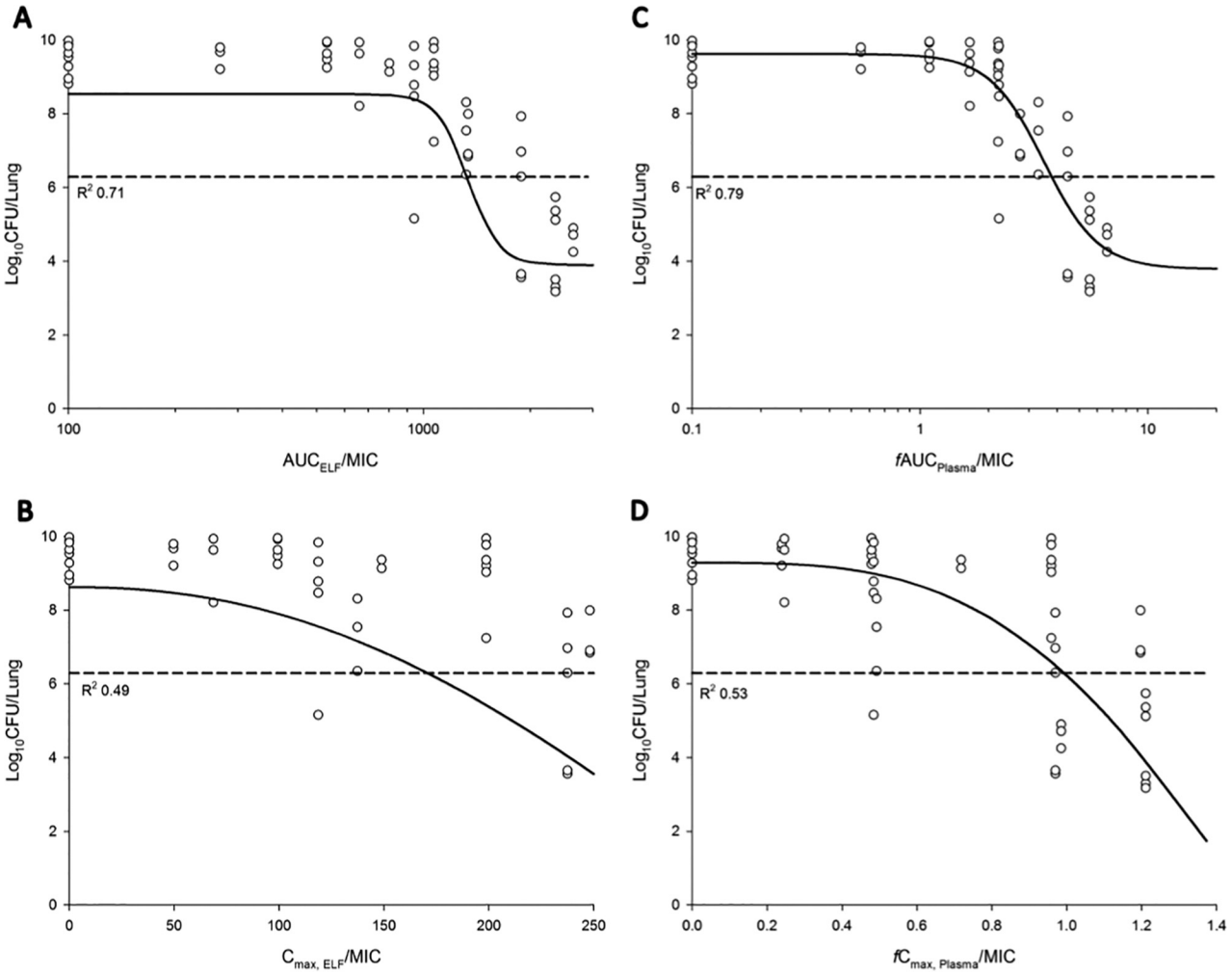

FIG 5 Relationship between the $\log_{10}$ CFU/lung of *P. aeruginosa* PAO1 at 24 h and the PK/PD indices for AUC_{ELF}/MIC (A), $C_{max,ELF}$/MIC (B), $fAUC_{Plasma}$/MIC (C), and $fC_{max\ Plasma}$/MIC (D). $\%T_{>MIC,ELF}$ and $\%fT_{>MIC,Plasma}$ could not be adequately examined. The broken line represents the average bacterial burden in the lungs at the start of aerosolized polymyxin B treatment.

Table 4. The AUC/MIC targets associated with bacteriostasis against the three *P. aeruginosa* strains were 1,326 to 1,506 in ELF and 3.14 to 4.03 in plasma.

Histopathological examination of the lungs following treatment with aerosolized polymyxin B in healthy and neutropenic infected mice. Table 5 shows the histopathological results of the mouse lungs following pulmonary administration of

TABLE 3 PK/PD model parameters for AUC_{ELF}/MIC and $fAUC_{plasma}$/MIC of aerosolized polymyxin B against three strains of *P. aeruginosa*

Strain and sample source	Value(s) (% RSE) for PK/PD parameter[a]:				
	E_{max} ($\log_{10}$ CFU/lung)	E_O ($\log_{10}$ CFU/lung)	EI_{50}	γ	R^2
ELF					
ATCC 27853	4.74 (11.6)	8.54 (3.26)	1340 (4.67)	9.99 (61.5)	0.70
PAO1	4.65 (10.8)	8.54 (3.21)	1,335 (4.60)	9.94 (59.7)	0.71
FADDI-PA022	4.34 (7.51)	8.54 (1.48)	1,528 (4.73)	9.02 (29.7)	0.88
Plasma					
ATCC 27853	6.61 (29.6)	9.06 (4.61)	3.35 (24.2)	2.80 (42.5)	0.70
PAO1	5.84 (19.9)	9.62 (2.71)	3.50 (15.0)	3.63 (33.3)	0.79
FADDI-PA022	4.70 (11.0)	8.63 (1.80)	3.61 (7.40)	5.13 (26.2)	0.87

[a] E_0 is the effect in the absence of polymyxin B treatment; E_{max} is the maximal effect; EI_{50} is the value of *f*AUC/MIC required to achieve 50% of E_{max}; γ is the Hill coefficient.

TABLE 4 Polymyxin B AUC_{ELF}/MIC and $fAUC_{plasma}$/MIC target values associated with bacteriostasis and 1- and 2-log_{10} kills[a]

Strain	Target value[b]		
	Stasis	1-log_{10} kill	2-log_{10} kill
AUC_{ELF}/MIC			
ATCC 27853	1,506 (1,337–1,951)	1,922 (1,422–2,663)	ND
PAO1	1,326 (1,213–1,448)	1,453 (1,315–1,773)	1,693 (1,410–2,558)
FADDI-PA022	1,416 (1,296–1,512)	1,573 (1,470–1,697)	1,778 (1,635–2,076)
$fAUC_{plsma}$/MIC			
ATCC 27853	4.03 (2.44–7.53)	5.24 (2.89–10.6)	ND
PAO1	3.78 (2.91–5.30)	4.68 (3.46–7.57)	6.70 (4.01–10.9)
FADDI-PA022	3.14 (2.72–3.51)	3.73 (3.32–4.26)	4.49 (3.89–5.74)

[a]Results show target values associated with bacteriostasis and 1- and 2-log_{10} kills against all three strains of *P. aeruginosa* in the mouse lung infection model.
[b]Values in parentheses are the 10th to 90th percentile ranges generated from Monte Carlo simulation. ND, not determined.

polymyxin B. Mice treated with saline showed no significant inflammation (SQS of $<+0.50$). Mice treated with the highest tolerable inhalable dose of polymyxin B (8.24 mg base/kg thrice daily or 10.3 mg base/kg twice daily) showed only minor inflammation (SQS of $+1.33$). At 24 h postdose, the infected lungs had necrosis and alveolar inflammation with infiltration of polymorphonuclear cells (SQS of $+2.00$) (Table 5). Following treatment with aerosolized polymyxin B (4.12 mg base/kg twice and thrice daily and 8.24 mg base/kg twice and thrice daily), inflammation was substantially reduced and the lung epithelium was mostly unaffected. Treatment with 4.12 mg base/kg polymyxin B thrice daily significantly reduced the SQS scoring to $+0.75$, indicating very minor damage.

DISCUSSION

Respiratory tract infections due to MDR *P. aeruginosa* are increasing and place a major burden on the global health care system (1). Over the last decade, inhalation of polymyxins has become a complementary practice for treating respiratory tract infections, such as those in patients with cystic fibrosis (29, 30) and ventilator-associated pneumonia (31–33). Recent preclinical and clinical PK/PD studies highlighted the advantage of aerosolized polymyxins over systemic administration in treating respiratory tract infections (12, 17–19, 22, 34, 35). However, the majority of PK/PD studies of

TABLE 5 Histopathological examination of lung toxicity in healthy and *P. aeruginosa*-infected mouse lungs 24 h after pulmonary administration of polymyxin B

Amt of polymyxin B (mg base/kg)	Dosing regimen	Histopathological result for:			
		Noninfected healthy mice		Neutropenic infected mice	
		n	Avg SQS	*n*	Avg SQS
Saline	Once daily	4	0.00	NA	NA
Saline	Twice daily	3	0.00	NA	NA
Saline	Thrice daily	4	+0.50	NA	NA
Growth control	NA[a]	NA	NA	8	+2.00
2.06	Once daily	3	+1.00	NA	NA
2.06	Twice daily	3	+1.00	NA	NA
2.06	Thrice daily	3	+0.33	NA	NA
4.12	Once daily	3	+1.00	4	+2.00
4.12	Twice daily	3	+1.33	4	+1.00
4.12	Thrice daily	3	+1.00	4	+0.75
8.24	Once daily	3	+1.00	4	+2.25
8.24	Twice daily	3	+1.00	3	+1.00
8.24	Thrice daily	3	+1.33	5	+1.40
10.3	Once daily	3	+0.67	NA	NA
10.3	Twice daily	3	+1.33	NA	NA

[a]NA, not applicable.

aerosolized polymyxins have focused on CMS/colistin, despite aerosolized polymyxin B also being used in the clinic (28). Give that the systemic PK differ between colistin and polymyxin B following systemic administration, it is necessary to examine the PK/PD of polymyxin B following pulmonary administration. Our study is the first to examine the PK/PD of aerosolized polymyxin B in a mouse lung infection model and to demonstrate that AUC_{ELF}/MIC and $fAUC_{Plasma}$/MIC was the most predictive PK/PD index of aerosolized polymyxin B (Fig. 5 and Table 3).

To investigate the PK of polymyxin B following pulmonary and intravenous administration, a population PK model was constructed (Fig. 4). The developed population PK model adequately predicted polymyxin B disposition following intravenous and pulmonary administration (Fig. 2 and 3). In our model, the absorption of polymyxin B into the systemic circulation following pulmonary administration is best described by the first-order rate constant (Fig. 4). Similar to aerosolized colistin (2.64 and 5.28 mg base/kg) in neutropenic lung-infected mice (26), the peak plasma concentration of unbound polymyxin B ($fC_{max,\ Plasma}$ of 0.46 $\pm$ 0.04 mg/liter) (Fig. 1 and Table 1) appeared rapidly after pulmonary administration, with a time to peak plasma concentration (T_{max}) of 15 min (for a dose of 4.12 mg base/kg). Despite the fast absorption of polymyxin B into the systemic circulation following pulmonary administration, the plasma $fC_{max,\ Plasma}$ value achieved after pulmonary administration was significantly lower than that at 15 min (0.84 $\pm$ 0.14 mg/liter) (Fig. 1) following intravenous administration (4.12 mg base/kg).

Based on the current PK model, most of the polymyxin B inhaled dose (~99.3% [SE of 6.89%]) (Table 2) was absorbed into systemic circulation. The bioavailability of aerosolized polymyxin B was very similar to the result obtained from an aerosolized colistin study in *P. aeruginosa*-infected mice (100%) (26) but was significantly higher than that in rats (31 to 69%) (18, 19, 36). The differences in the observed bioavailability among different species are likely due to differential expression of the peptide transporter PEPT2 in lung epithelial cells (37). PEPT2 has recently been identified to be responsible for the uptake of polymyxins in human embryonic kidney 293 (HEK293) cells (38). Given that PEPT2 is abundantly expressed in the airway epithelium (37, 39), it may have a significant impact on the disposition of polymyxins (18). The expression level of PEPT2 mRNA in mouse lungs is approximately 2-fold higher than that in rat lungs (40). Unfortunately, interspecies differences between the expression level of PEPT2 of mice and humans is unknown (41). It should be noted, however, that the mouse and human PEPT2 have a similar structure (sequence homology of 80%) (41) and that both are able to transport the same range of substrates (42, 43). In a recent PK study following pulmonary administration of colistin to rats (18), a nonlinear (Michaelis-Menten) model was incorporated to describe the transfer of colistin across the lung epithelium. In the current study, the incorporation of Michaelis-Menten kinetics to describe the transfer of polymyxin B from ELF to plasma did not provide a significant improvement in the PK model. Although the role of PEPT2 in transporting polymyxins has been verified in HEK293 cells (38) and supported by PK modeling in rats (18), its roles in mice remain unclear. Further studies are being conducted in our laboratory.

A two-compartment PK model was required to describe the disposition of polymyxin B in ELF following pulmonary administration (Fig. 4). The ELF1 compartment potentially represents a depot for polymyxin B in the upper airway from which the drug is bidirectionally transferred to peripheral lung regions and, to some extent, the lung epithelial cells. In the current study, the apparent volume of the epithelial lining fluid (V_{ELF}) was estimated in the proposed population PK model, and interestingly, the estimated V_{ELF} value (named V_{E1} in Table 2) was relatively larger than the calculated V_{ELF} using the urea dilution method. In compartmental PK analysis, an estimated V_{ELF} has no real physiological meaning (21). The relatively large estimated V_{E1} and V_{E2} values (0.0149 liters/kg; SE of 14.5%) indicate significant binding of polymyxin B in the lungs (e.g., to mucin, surfactants, and lung epithelial cells).

Similar to the observations from the colistin PK study (18, 19, 26), the polymyxin B

concentration in ELF was affected by the route of administration. In contrast to the high polymyxin B exposure in ELF (AUC_{ELF} of ~600 mg · h/liter for 4.12 mg base/kg) (Table 1) following pulmonary delivery, polymyxin B was undetectable in ELF following intravenous administration (Fig. 1 and Table 1). The population PK model developed here provides an opportunity to simulate the undetectable ELF polymyxin B concentration following intravenous administration. It is important to note that the LOQ for polymyxin B in ELF is ~2.00 mg/liter in our study, and the ELF concentrations simulated by the PK model after intravenous administration of polymyxin B (4.12 mg base/kg) remained below the ELF LOQ.

Our study in neutropenic infected mice demonstrates that inhalation of polymyxin B achieved prolonged and extensive pulmonary exposure (Fig. 1). High pulmonary exposure to polymyxin B was maintained above the resistance breakpoints (>2 mg/liter) against *P. aeruginosa* and *A. baumannii* over the 12-h sampling period (44). The retention of polymyxin B in ELF was proposed to be due to the binding of polymyxin B to alveolar macrophages (45) and the alveolar basement membrane (46) via electrostatic interactions (47). Similar mechanisms were also suggested for the prolonged and extensive exposure observed in ELF following pulmonary administration of colistin in sheep (35), rats (36), and mice (26). The exact mechanism for the polymyxin retention in ELF is not known, and further studies are warranted.

Collectively, the PK results suggest that aerosolized polymyxin B is as effective as aerosolized colistin. It should be noted that colistin in clinical practice is administered in the form of a prodrug, CMS. In a rat PK study following pulmonary administration of CMS, only 23 to 39% of the dose converted to colistin in the rat lungs (17, 19). Furthermore, the CMS-to-colistin conversion process is slow and the T_{max} of the formed colistin is only achieved at 1 to 5 h after nebulization in patients with cystic fibrosis (12). On the contrary, polymyxin B is administered in its active form, hence, therapeutic efficacy can be rapidly attained (Fig. 1).

AUC_{ELF}/MIC and $fAUC_{plasma}$/MIC were identified as the most predictive PK/PD indices to describe the antimicrobial efficacy of aerosolized polymyxin B against MDR *P. aeruginosa* in the mouse lung infection model (Fig. 5 and Table 3). A relatively low degree of interstrain variability (<1-fold) in AUC_{ELF}/MIC and $fAUC_{plasma}$/MIC was observed for all three strains of *P. aeruginosa* (Table 4). The $fAUC_{plasma}$/MIC target values associated with various killing effects for aerosolized polymyxin B (Table 4) compared well with those obtained in aerosolized colistin studies using the same strains in a mouse lung infection model (26). Unlike the $fAUC_{plasma}$/MIC, the AUC_{ELF}/MIC of polymyxin B differs from that observed previously in the colistin PK/PD study (26). The AUC_{ELF}/MIC of polymyxin B to achieve bacteriostasis against *P. aeruginosa* was 1,326 to 1,506 (Table 4), which is much higher than the AUC_{ELF}/MIC of colistin (684 to 1,050) (26), even after accounting for the difference in molecular weights. The differences could be interpreted in terms of the different binding affinities to lung surfactants and plasma between polymyxin B and colistin. Polymyxin B (82.3% ± 4.30% and 68.4% ± 3.50% for polymyxin B1 and polymyxin B2, respectively) was found to display much higher plasma protein binding than colistin (56.6% ± 9.25% and 41.7% ± 12.4% for colistin A and colistin B, respectively) in rat plasma (48). Structurally, polymyxin B contains a D-phenylalanine residue at position 6 as opposed to a D-leucine residue at position 6 of colistin (4). The much higher plasma protein binding properties of polymyxin B very likely is due to the higher hydrophobicity of D-phenylalanine compared to D-leucine (49). Based on the structural differences, polymyxin B and colistin are likely to have different binding affinities to pulmonary surfactants, proteins, mucin, and lung epithelium in the ELF, hence the differences in AUC_{ELF}/MIC observed. Future studies to examine the binding of polymyxin B to substances in ELF are needed. Another noticeable difference between the two studies was that unlike the colistin PK/PD study, in which a 2-log_{10} kill was not achieved for any of the three strains (26), in the current study, a 2-log_{10} kill was achieved for strains PAO1 and FADDI-PA022 but not for ATCC 27853 (Table 4).

An exciting finding was that the target AUC_{ELF}/MIC to achieve stasis and 1- and

2-$\log_{10}$ reductions in bacterial loads was 100 times higher than the MICs for all three *P. aeruginosa* strains. This higher-than-expected AUC_{ELF}/MIC target was proposed to be linked to the presence of multiple purulent plugs obstructing bronchioles, which prevented aerosolized polymyxin B from accessing all sites of infection (34). This phenomenon was noted in *P. aeruginosa*-infected piglets in which the deposition of a colistin aerosol was significantly impaired in deep airway infections (34). It could also be due to the presence of mucin (50) and a pulmonary surfactant (51). An *in vitro* study has shown significant impairment of the antimicrobial activity of polymyxins as a result of the interaction with porcine lung surfactants (51). Finally, the Penn-Century MicroSprayer used for pulmonary administration generates aerosol droplets with a size of >10 μm (17), which may result in a heterogeneous disposition of polymyxin B in the lungs.

Due to toxicity concerns and technical difficulties in pulmonary administration, traditional dose fractionation experiments could not be reliably performed in the present study. As mice were unable to tolerate >10.3 mg base/kg aerosolized polymyxin B in a single dose or a cumulative dose of 24.8 mg base/kg, a modified dose fractionation study was conducted. Nevertheless, much better correlations were observed between the killing effect and AUC_{ELF}/MIC (R^2 of 0.70 to 0.88) than with $C_{max,\ ELF}$/MIC (R^2 of 0.49 to 0.58) and, similarly, killing effect versus AUC_{Plasma}/MIC (R^2 of 0.70 to 0.87) than with $C_{max,\ Plasma}$/MIC ($R^2 = 0.53$ to 0.60) (Fig. 5 and Table 3). Due to the limited tolerance, the sigmoid dose-response relationship could not be fully characterized for aerosolized polymyxin B. In addition, for easy comparisons with aerosolized colistin PK/PD, the same bacterial isolates (polymyxin B MICs of 1 mg/liter) were examined in the present study (26, 52). In light of the interspecies differences, translation of the calculated PK/PD targets from mouse to human needs to be verified in future clinical studies.

A potential advantage of pulmonary administration of polymyxin B in treating respiratory tract infections was also supported by the histopathological results (Table 5). Severe lung infection resulted in inflammation and tissue necrosis, with a corresponding SQS of +2 (Table 5). In lung infections caused by *P. aeruginosa*, lipopolysaccharide (LPS), an endotoxin released by bacteria, can induce severe lung damage and inflammation (53). In addition to the antimicrobial effect, polymyxin B exhibits an LPS-neutralizing effect (53, 54). Aerosolized polymyxin B reduced the lung inflammation when multiple dosage regimens were utilized (Table 5). The treatment with the highest tolerable aerosolized polymyxin B dose (8.24 mg base/kg thrice daily) was able to protect the lung epithelium and reduced the inflammation at 24 h posttreatment (SQS of +1.40) (Table 5). Potential toxicity of aerosolized polymyxin B was also examined in healthy mice (Table 5). The pulmonary delivery resulted in minor lung inflammation, which was comparable to the results of colistin administration but slightly worse than that obtained after the administration of CMS (26). These results suggest that aerosolized polymyxin B is relatively safe to use for treating respiratory tract infections.

To the best of our knowledge, this is the first population PK model that describes the disposition of polymyxin B in both ELF and plasma in mice following pulmonary and intravenous administration. This study highlights the distinct advantage of pulmonary delivery of polymyxin B in achieving high drug exposures in ELF over intravenous administration. Furthermore, AUC_{ELF}/MIC and $fAUC_{plasma}$/MIC were identified as the most predictive PK/PD indices that describe the antimicrobial efficacy of aerosolized polymyxin B against *P. aeruginosa* in a mouse lung infection model. We also determined the AUC_{ELF}/MIC and $fAUC_{plasma}$/MIC targets associated with various magnitudes of bacterial kill. The potential advantage of pulmonary delivery of polymyxin B is also supported by the safety results. Ultimately, the PK model and PK/PD targets provide important information for optimizing the inhalation of polymyxin B to maximize its antimicrobial efficacy while minimizing any potential toxicity.

MATERIALS AND METHODS

Chemicals and bacterial strains. Polymyxin B was purchased from Sigma-Aldrich (St. Louis, MO, USA), and solutions were freshly prepared in sterile 0.9% saline (52). Three strains of *P. aeruginosa* were

examined: two reference strains, ATCC 27853 and PAO1, and one MDR clinical isolate, FADDI-PA022 (MIC of 1 mg/liter for all three strains). MICs were determined using the broth microdilution method in cation-adjusted Mueller-Hinton broth (CAMHB) (55) without polysorbate 80 or mucin.

PK of aerosolized and intravenous polymyxin B in neutropenic infected mice. All animal experiments were approved by the Monash Institute of Pharmaceutical Sciences Animal Ethics Committee and conducted in accordance with the Australian Code of Practice for the Care and Use of Animals for Scientific Purposes. Female Swiss mice (6 to 8 weeks, weight of 30 to 35 g) were employed (Monash Animal Research Platform, Victoria, Australia) in the neutropenic mouse lung infection model (26). A Penn-Century MicroSprayer (model IA-1C; Penn-Century, Philadelphia, PA, USA) was used to deliver 25 μl of bacterial suspension (approximately 10^6 bacterial cells in the early logarithmic phase) directly into the lungs (56). Aerosolized polymyxin B treatment began 2 h after bacterial inoculation.

Single-dose PK studies were conducted in neutropenic lung-infected mice following administration of polymyxin B by inhalation (4.12 and 8.24 mg base/kg, volume of 25 μl) or intravenously (4.12 mg base/kg, volume of 50 μl). The maximum dosage regimens for intravenous and pulmonary administration of polymyxin B were chosen based upon the tolerability in mice. The lowest pulmonary dosage regimen was selected considering the LOQ of the analytical method for polymyxin B in plasma samples. For the pulmonary dosing study, plasma and bronchoalveolar lavage fluid (BALF) were collected at 15 and 30 min and at 1, 2, 3, 4, 6, and 12 h postdose ($n = 4$ per time point). For the intravenous dosing study, plasma and BALF were collected at 5, 15, and 30 min and 1, 1.5, 2, 3, and 6 h postdose ($n = 4$ per time point). Bronchoalveolar lavage was performed using 0.5 ml of 0.9% saline for two cycles, and for each animal the recovered BALF fractions were pooled. The BALF and plasma samples from each animal were stored separately, and the concentrations were determined by a validated liquid chromatography-tandem mass spectrometry (LC-MS/MS) assay, with minor modifications (57). Briefly, the BALF and plasma samples were deproteinized with 0.1% formic acid in acetonitrile and centrifuged at 18,210 $\times$ *g* for 15 min. The calibration curve ranged from 0.10 mg/liter to 10.0 mg/liter for plasma and 0.10 mg/liter to 8.00 mg/liter for BALF. The LOQ for BALF and plasma was 0.10 mg/liter. The assay accuracies in BALF and plasma were $<$11.0% and $<$14.8%, respectively.

Urea was used to determine the apparent volume of the epithelial lining fluid (V_{ELF}) (58). Urea concentrations in both BALF and plasma were determined using a QuantiChrom urea assay kit (BioAssay Systems, California, USA). V_{ELF} was calculated as $V_{ELF} = [\text{urea}]_{BALF}/[\text{urea}]_{Plasma} \times V_{BALF}$, where $[\text{urea}]_{Plasma}$, $[\text{urea}]_{BALF}$, and V_{BALF} are urea concentration (milligrams per decaliter) in plasma and BALF and recovered BALF volume, respectively.

The apparent polymyxin B concentration for each animal in V_{ELF} was calculated by multiplying the polymyxin B concentration in BALF by the ratio of urea concentration in plasma and BALF as $[\text{polymyxin B}]_{ELF} = [\text{polymyxin B}]_{BALF} \times [\text{urea}]_{Plasma}/[\text{urea}]_{BALF}$.

Population PK modeling. Noncompartmental (NCA) PK parameters (Phoenix WinNonlin software, version 6.3; Pharsight Corporation) were used as an initial estimate to guide the development of a population PK model (see Fig. S1 in the supplemental material). Initially, the model was independently developed for polymyxin B concentrations in plasma and ELF following intravenous or pulmonary administration. Subsequently, the ELF and plasma concentrations after pulmonary or intravenous administration were simultaneously analyzed using a Monte Carlo parametric expectation maximization algorithm (importance sampling, pmethod of 4) in S-ADAPT (version 1.57) facilitated by S-ADAPT TRAN (59). The Akaike information criterion (AIC), Bayesian information criterion (BIC) values, and visual inspection of the diagnostic plots (i.e., observed versus population-fitted concentration plots) and fitted functions were used to guide the selection of the best model to describe the observed data. In addition, the objective function (reported as $-1\times$ log likelihood in S-ADAPT) was employed to discriminate between the nested models; a decrease in the objective function of 1.92 U (chi-square test, with one degree of freedom) was considered significant. The final polymyxin B population PK model was evaluated using a visual predictive check (60).

The population PK model was built with a reduced data set (i.e., the data set without outliers) (61). Suspected outlier observations were tested, and if significant, outliers were excluded based on the following criteria. Data points were considered outliers if weighted residuals were greater than 3 to 5 standard deviation units and their exclusion changed the fitted function. For the case in which the exclusion of outliers significantly improved the fitted function and the precision of the estimates, the outliers were excluded from the final population PK model. The residual unexplained variability in both plasma and ELF was evaluated using additive and proportional errors, which were fixed to the assay precision and LOQ. Plasma drug concentrations below the LOQ were included using the Beal M3 method (62).

PK/PD of aerosolized polymyxin B. Neutropenic mice infected with *P. aeruginosa* ATCC 27853, PAO1, and FADDI-PA022 were treated with aerosolized polymyxin B 2 h after bacterial inoculation. Dose fractionation studies were performed; the dosage regimens involved once-daily administration of 2.06, 4.12, 6.18, 8.24, and 10.3 mg base/kg, twice-daily administration of 4.12, 8.24, and 10.3 mg base/kg, and thrice-daily administration of 4.12 and 8.24 mg base/kg. Lungs were aseptically harvested at 24 h after dosing, homogenized with 8 ml of 0.9% saline, and filtered through a sterile filter bag (bag stomacher filter, sterile; pore size, 280 μm; 0.5 by 16 cm; Labtek Pty Ltd., QLD, Australia). Filtrate samples were serially diluted with 0.9% saline and spiral plated on nutrient agar plates to determine bacterial load in the lungs. Bacterial loads were expressed as the $\log_{10}$ CFU per lung, and the limit of counting was 164 CFU/lung (equivalent to one colony per plate). A nonmechanistic approach was employed to calculate the PK/PD index of aerosolized polymyxin B for the treatment of respiratory tract infections using model-predicted PK parameters (Fig. S1). The principle of superposition was applied to single-dose PK

and unbound concentration-time profiles to obtain the corresponding PK parameters (fC_{max}, fAUC, and $fT_{>MIC}$) for multiple dosage regimens (26, 52). Subsequently, the inhibitory sigmoid dose-effect model was fitted to the PK/PD data to estimate the PK/PD indices for plasma and ELF (i.e., fAUC/MIC, fC_{max}/MIC, and $\%fT_{>MIC}$). The magnitude of various killing effects was assessed for the most predictive PK/PD index using the nonlinear least-squares regression analysis (63). Monte Carlo simulation ($n > 10{,}000$) was employed to estimate the 10th and 90th percentile range for the PK/PD target.

Histopathological examination. Histopathological examinations of lungs were performed in healthy and neutropenic lung infected mice with aerosolized polymyxin B. The dosage regimens involved once-, twice-, and thrice-daily administration of polymyxin B at 2.06, 4.12, 8.24, and 10.3 mg base/kg. Due to profound toxicity, the largest total daily dose administered was 24.8 mg base/kg. At 24 h following pulmonary administration, mice were humanely killed and lungs were harvested and fixed in formalin immediately. To avoid any potential artificial damage to the lung epithelium, bronchoalveolar lavage and cardiac puncture were not performed. A semiquantitative scoring (SQS) system was adapted to quantify the extent of lung damage (64). Briefly, we used the following grades for the severity and nature of the histopathological changes in the lungs: grade 0, no changes or mild changes considered insignificant; grade 1, minimal lesions affecting 1 to 25% of the area; grade 2, multifocal lesions affecting 25 to 50% of the area; and grade 3, severe tissue changes affecting >50% of the area. The grades were given the following scores: grade 0, 0.1; grade 1, 1; grade 2, 4; and grade 3, 10. Percentages of damage across different levels of the lungs were given the following scores: <1%, 0; from 1 to <5%, 1; from 5 to <10%, 2; from 10 to <20%, 3; from 20 to <30%, 4; from 30 to <40%, 5; ≥40%, 6. The overall lung histology score was determined as the product of the grade and percent damage score. An SQS was assigned the following scores: SQS 0, no significant change; SQS +1, mild damage; SQS +2, mild to moderate damage; SQS +3, moderate damage; SQS +4, moderate to severe damage; and SQS +5, severe damage.

SUPPLEMENTAL MATERIAL

Supplemental material for this article may be found at https://doi.org/10.1128/AAC.00211-17.

SUPPLEMENTAL FILE 1, PDF file, 0.6 MB.

ACKNOWLEDGMENTS

We acknowledge financial support from the National Health and Medical Research Council's (NHMRC) project grant (APP1065046). J.L. and A.F. are supported by research grants from the National Institute of Allergy and Infectious Diseases (NIAID) of the National Institutes of Health (NIH; R01 AI111965). Y.-W.L. is a recipient of the Australian Postgraduate Award. J.L. is an Australian NHMRC Senior Research Fellow.

The content is solely the responsibility of the authors and does not necessarily represent the official views of the National Institute of Allergy and Infectious Diseases or the National Institutes of Health.

This study utilized the Australian Phenomics Network Histopathology and Organ Pathology Service at the University of Melbourne.

REFERENCES

1. Bodey GP, Bolivar R, Fainstein V, Jadeja L. 1983. Infections caused by Pseudomonas aeruginosa. Rev Infect Dis 5:279–313. https://doi.org/10.1093/clinids/5.2.279.
2. Zavascki AP, Goldani LZ, Li J, Nation RL. 2007. Polymyxin B for the treatment of multidrug-resistant pathogens: a critical review. J Antimicrob Chemother 60:1206–1215. https://doi.org/10.1093/jac/dkm357.
3. Li J, Nation RL, Turnidge JD, Milne RW, Coulthard K, Rayner CR, Paterson DL. 2006. Colistin: the re-emerging antibiotic for multidrug-resistant Gram-negative bacterial infections. Lancet Infect Dis 6:589–601. https://doi.org/10.1016/S1473-3099(06)70580-1.
4. Kwa A, Kasiakou SK, Tam VH, Falagas ME. 2007. Polymyxin B: similarities to and differences from colistin (polymyxin E). Expert Rev Anti Infect Ther 5:811–821. https://doi.org/10.1586/14787210.5.5.811.
5. Bergen PJ, Li J, Rayner CR, Nation RL. 2006. Colistin methanesulfonate is an inactive prodrug of colistin against Pseudomonas aeruginosa. Antimicrob Agents Chemother 50:1953–1958. https://doi.org/10.1128/AAC.00035-06.
6. Nation RL, Velkov T, Li J. 2014. Colistin and polymyxin B: peas in a pod, or chalk and cheese? Clin Infect Dis 59:88–94. https://doi.org/10.1093/cid/ciu213.
7. Karvanen M, Plachouras D, Friberg LE, Paramythiotou E, Papadomichelakis E, Karaiskos I, Tsangaris I, Armaganidis A, Cars O, Giamarellou H. 2013. Colistin methanesulfonate and colistin pharmacokinetics in critically ill patients receiving continuous venovenous hemodiafiltration. Antimicrob Agents Chemother 57:668–671. https://doi.org/10.1128/AAC.00985-12.
8. Karaiskos I, Friberg LE, Pontikis K, Ioannidis K, Tsagkari V, Galani L, Kostakou E, Baziaka F, Paskalis C, Koutsoukou A. 2015. Colistin population pharmacokinetics after application of a loading dose of 9 MU colistin methanesulfonate in critically ill patients. Antimicrob Agents Chemother 59:7240–7248. https://doi.org/10.1128/AAC.00554-15.
9. Plachouras D, Karvanen M, Friberg LE, Papadomichelakis E, Antoniadou A, Tsangaris I, Karaiskos I, Poulakou G, Kontopidou F, Armaganidis A, Cars O, Giamarellou H. 2009. Population pharmacokinetic analysis of colistin methanesulfonate and colistin after intravenous administration in critically ill patients with infections caused by gram-negative bacteria. Antimicrob Agents Chemother 53:3430–3436. https://doi.org/10.1128/AAC.01361-08.
10. Garonzik SM, Li J, Thamlikitkul V, Paterson DL, Shoham S, Jacob J, Silveira FP, Forrest A, Nation RL. 2011. Population pharmacokinetics of colistin methanesulfonate and formed colistin in critically ill patients from a multicenter study provide dosing suggestions for various categories of patients. Antimicrob Agents Chemother 55:3284–3294. https://doi.org/10.1128/AAC.01733-10.

11. Sandri AM, Landersdorfer CB, Jacob J, Boniatti MM, Dalarosa MG, Falci DR, Behle TF, Bordinhao RC, Wang J, Forrest A, Nation RL, Li J, Zavascki AP. 2013. Population pharmacokinetics of intravenous polymyxin B in critically ill patients: implications for selection of dosage regimens. Clin Infect Dis 57:524–531. https://doi.org/10.1093/cid/cit334.
12. Yapa WS, Li J, Patel K, Wilson JW, Dooley MJ, George J, Clark D, Poole S, Williams E, Porter CJ, Nation RL, McIntosh MP. 2014. Pulmonary and systemic pharmacokinetics of inhaled and intravenous colistin methanesulfonate in cystic fibrosis patients: targeting advantage of inhalational administration. Antimicrob Agents Chemother 58:2570–2579. https://doi.org/10.1128/AAC.01705-13.
13. Cheah S-E, Li J, Tsuji BT, Forrest A, Bulitta JB, Nation RL. 2016. Colistin and polymyxin B dosage regimens against Acinetobacter baumannii: differences in activity and the emergence of resistance. Antimicrob Agents Chemother 60:3921–3933. https://doi.org/10.1128/AAC.02927-15.
14. Zavascki AP, Goldani LZ, Cao G, Superti SV, Lutz L, Barth AL, Ramos F, Boniatti MM, Nation RL, Li J. 2008. Pharmacokinetics of intravenous polymyxin B in critically ill patients. Clin Infect Dis 47:1298–1304. https://doi.org/10.1086/592577.
15. Hartzell JD, Neff R, Ake J, Howard R, Olson S, Paolino K, Vishnepolsky M, Weintrob A, Wortmann G. 2009. Nephrotoxicity associated with intravenous colistin (colistimethate sodium) treatment at a tertiary care medical center. Clin Infect Dis 48:1724–1728. https://doi.org/10.1086/599225.
16. Nation RL, Garonzik SM, Thamlikitkul V, Giamarellos-Bourboulis EJ, Forrest A, Paterson DL, Li J, Silveira FP. 2016. Dosing guidance for intravenous colistin in critically-ill patients. Clin Infect Dis 64:565–571.
17. Marchand S, Gobin P, Brillault J, Baptista S, Adier C, Olivier J-C, Mimoz O, Couet W. 2010. Aerosol therapy with colistin methanesulfonate: a biopharmaceutical issue illustrated in rats. Antimicrob Agents Chemother 54:3702–3707. https://doi.org/10.1128/AAC.00411-10.
18. Gontijo AVL, Grégoire N, Lamarche I, Gobin P, Couet W, Marchand S. 2014. Biopharmaceutical characterization of nebulized antimicrobial agents in rats: 2. Colistin. Antimicrob Agents Chemother 58:3950–3956. https://doi.org/10.1128/AAC.02819-14.
19. Yapa WS, Li J, Porter CJ, Nation RL, Patel K, McIntosh MP. 2013. Population pharmacokinetics of colistin methanesulfonate in rats: achieving sustained lung concentrations of colistin for targeting respiratory infections. Antimicrob Agents Chemother 57:5087–5095. https://doi.org/10.1128/AAC.01127-13.
20. Ratjen F, Rietschel E, Kasel D, Schwiertz R, Starke K, Beier H, Van Koningsbruggen S, Grasemann H. 2006. Pharmacokinetics of inhaled colistin in patients with cystic fibrosis. J Antimicrob Chemother 57:306–311. https://doi.org/10.1093/jac/dki461.
21. Boisson M, Jacobs M, Grégoire N, Gobin P, Marchand S, Couet W, Mimoz O. 2014. Comparison of intrapulmonary and systemic pharmacokinetics of colistin methanesulfonate (CMS) and colistin after aerosol delivery and intravenous administration of CMS in critically ill patients. Antimicrob Agents Chemother 58:7331–7339. https://doi.org/10.1128/AAC.03510-14.
22. Marchand S, Bouchene S, de Monte M, Guilleminault L, Montharu J, Cabrera M, Grégoire N, Gobin P, Diot P, Couet W. 2015. Pharmacokinetics of colistin methansulphonate (CMS) and colistin after CMS nebulisation in baboon monkeys. Pharm Res 32:3403–3414. https://doi.org/10.1007/s11095-015-1716-0.
23. Athanassa ZE, Markantonis SL, Fousteri M-ZF, Myrianthefs PM, Boutzouka EG, Tsakris A, Baltopoulos GJ. 2012. Pharmacokinetics of inhaled colistimethate sodium (CMS) in mechanically ventilated critically ill patients. Intensive Care Med 38:1779–1786. https://doi.org/10.1007/s00134-012-2628-7.
24. Nakwan N, Lertpichaluk P, Chokephaibulkit K, Villani P, Regazzi M, Imberti R. 2015. Pulmonary and systemic pharmacokinetics of colistin following a single dose of nebulized colistimethate in mechanically ventilated neonates. Pediatr Infect Dis J 34:961–963. https://doi.org/10.1097/INF.0000000000000775.
25. Gunderson BW, Ibrahim KH, Hovde LB, Fromm TL, Reed MD, Rotschafer JC. 2003. Synergistic activity of colistin and ceftazidime against multiantibiotic-resistant Pseudomonas aeruginosa in an in vitro pharmacodynamic model. Antimicrob Agents Chemother 47:905–909. https://doi.org/10.1128/AAC.47.3.905-909.2003.
26. Lin Y-W, Zhou Q, Cheah S-E, Zhao J, Chen K, Wang J, Chan H-K, Li J. 2017. Pharmacokinetics/pharmacodynamics of pulmonary delivery of colistin against Pseudomonas aeruginosa in a mouse lung infection model. Antimicrob Agents Chemother 61:e02025-16. https://doi.org/10.1128/AAC.02025-16.
27. Velkov T, Rahim NA, Zhou QT, Chan H-K, Li J. 2015. Inhaled anti-infective chemotherapy for respiratory tract infections: successes, challenges and the road ahead. Adv Drug Deliv Rev 85:65–82. https://doi.org/10.1016/j.addr.2014.11.004.
28. Pereira GH, Muller PR, Levin AS. 2007. Salvage treatment of pneumonia and initial treatment of tracheobronchitis caused by multidrug-resistant Gram-negative bacilli with inhaled polymyxin B. Diagn Microbiol Infect Dis 58:235–240. https://doi.org/10.1016/j.diagmicrobio.2007.01.008.
29. Jensen T, Pedersen SS, Garne S, Heilmann C, Høiby N, Koch C. 1987. Colistin inhalation therapy in cystic fibrosis patients with chronic Pseudomonas aeruginosa lung infection. J Antimicrob Chemother 19:831–838. https://doi.org/10.1093/jac/19.6.831.
30. Hansen C, Pressler T, Høiby N. 2008. Early aggressive eradication therapy for intermittent Pseudomonas aeruginosa airway colonization in cystic fibrosis patients: 15 years experience. J Cyst Fibros 7:523–530. https://doi.org/10.1016/j.jcf.2008.06.009.
31. Chastre J, Fagon J-Y. 2002. Ventilator-associated pneumonia. Am J Respir Crit Care Med 165:867–903. https://doi.org/10.1164/ajrccm.165.7.2105078.
32. Michalopoulos A, Kasiakou SK, Mastora Z, Rellos K, Kapaskelis AM, Falagas ME. 2005. Aerosolized colistin for the treatment of nosocomial pneumonia due to multidrug-resistant Gram-negative bacteria in patients without cystic fibrosis. Crit Care 9:R53–R59. https://doi.org/10.1186/cc3020.
33. Mubareka S, Rubinstein E. 2005. Aerosolized colistin for the treatment of nosocomial pneumonia due to multidrug-resistant Gram-negative bacteria in patients without cystic fibrosis. Crit Care 9:29–30.
34. Lu Q, Girardi C, Zhang M, Bouhemad B, Louchahi K, Petitjean O, Wallet F, Becquemin M-H, Le Naour G, Marquette C-H. 2010. Nebulized and intravenous colistin in experimental pneumonia caused by Pseudomonas aeruginosa. Intensive Care Med 36:1147–1155. https://doi.org/10.1007/s00134-010-1879-4.
35. Landersdorfer CB, Nguyen T-H, Lieu LT, Nguyen G, Bischof RJ, Meeusen EN, Li J, Nation RL, McIntosh MP. 2017. Substantial targeting advantage achieved by pulmonary administration of colistin methanesulfonate in a large-animal model. Antimicrob Agents Chemother 61:e01934-16. https://doi.org/10.1128/AAC.01934-16.
36. Yapa SW. 2013. Ph.D. thesis. Monash University, Melbourne, Victoria, Australia.
37. Bosquillon C. 2010. Drug transporters in the lung–do they play a role in the biopharmaceutics of inhaled drugs? J Pharm Sci 99:2240–2255. https://doi.org/10.1002/jps.21995.
38. Lu X, Chan T, Xu C, Zhu L, Zhou QT, Roberts KD, Chan H-K, Li J, Zhou F. 2016. Human oligopeptide transporter 2 (PEPT2) mediates cellular uptake of polymyxins. J Antimicrob Chemother 71:403–412. https://doi.org/10.1093/jac/dkv340.
39. Saito H, Terada T, Okuda M, Sasaki S, Inui K-I. 1996. Molecular cloning and tissue distribution of rat peptide transporter PEPT2. Biochim Biophys Acta 1280:173–177. https://doi.org/10.1016/0005-2736(96)00024-7.
40. Lu H, Klaassen C. 2006. Tissue distribution and thyroid hormone regulation of Pept1 and Pept2 mRNA in rodents. Peptides 27:850–857. https://doi.org/10.1016/j.peptides.2005.08.012.
41. Kamal MA, Keep RF, Smith DE. 2008. Role and relevance of PEPT2 in drug disposition, dynamics, and toxicity. Drug Metab Pharmacokinet 23:236–242. https://doi.org/10.2133/dmpk.23.236.
42. Ganapathy ME, Brandsch M, Prasad PD, Ganapathy V, Leibach FH. 1995. Differential recognition of β-lactam antibiotics by intestinal and renal peptide transporters, PEPT 1 and PEPT 2. J Biol Chem 270:25672–25677. https://doi.org/10.1074/jbc.270.43.25672.
43. Sugawara M, Huang W, Fei YJ, Leibach FH, Ganapathy V, Ganapathy ME. 2000. Transport of valganciclovir, a ganciclovir prodrug, via peptide transporters PEPT1 and PEPT2. J Pharm Sci 89:781–789. https://doi.org/10.1002/(SICI)1520-6017(200006)89:6<781::AID-JPS10>3.0.CO;2-7.
44. Gales AC, Jones RN, Sader HS. 2011. Contemporary activity of colistin and polymyxin B against a worldwide collection of Gram-negative pathogens: results from the SENTRY Antimicrobial Surveillance Program (2006-09). J Antimicrob Chemother 66:2070–2074. https://doi.org/10.1093/jac/dkr239.
45. Bysani GK, Stokes DC, Fishman M, Shenep JL, Hildner WK, Rufus K, Bradham N, Costlow ME. 1990. Binding of polymyxin B to rat alveolar macrophages. J Infect Dis 162:939–943. https://doi.org/10.1093/infdis/162.4.939.
46. Brody JS, Vaccaro CA, Hill NS, Rounds S. 1984. Binding of charged ferritin to alveolar wall components and charge selectivity of macromolecular

transport in permeability pulmonary edema in rats. Circ Res 55:155–167. https://doi.org/10.1161/01.RES.55.2.155.
47. Kunin CM, Bugg A. 1971. Binding of polymyxin antibiotics to tissues: the major determinant of distribution and persistence in the body. J Infect Dis 124:394–400. https://doi.org/10.1093/infdis/124.4.394.
48. Sivanesan S, Roberts K, Wang J, Chea S-E, Thompson PE, Li J, Nation RL, Velkov T. 2017. Pharmacokinetics of the individual major components of polymyxin B and colistin in rats. J Nat Prod 80:225–229. https://doi.org/10.1021/acs.jnatprod.6b01176.
49. Wimley WC, White SH. 1996. Experimentally determined hydrophobicity scale for proteins at membrane interfaces. Nat Struct Mol Biol 3:842–848. https://doi.org/10.1038/nsb1096-842.
50. Huang JX, Blaskovich MA, Pelingon R, Ramu S, Kavanagh A, Elliott AG, Butler MS, Montgomery AB, Cooper MA. 2015. Mucin binding reduces colistin antimicrobial activity. Antimicrob Agents Chemother 59:5925–5931. https://doi.org/10.1128/AAC.00808-15.
51. Schwameis R, Erdogan-Yildirim Z, Manafi M, Zeitlinger M, Strommer S, Sauermann R. 2013. Effect of pulmonary surfactant on antimicrobial activity in vitro. Antimicrob Agents Chemother 57:5151–5154. https://doi.org/10.1128/AAC.00778-13.
52. Cheah S-E, Wang J, Turnidge JD, Li J, Nation RL. 2015. New pharmacokinetic/pharmacodynamic studies of systemically administered colistin against Pseudomonas aeruginosa and Acinetobacter baumannii in mouse thigh and lung infection models: smaller response in lung infection. J Antimicrob Chemother 70:3291–3297.
53. Aoki N, Tateda K, Kikuchi Y, Kimura S, Miyazaki C, Ishii Y, Tanabe Y, Gejyo F, Yamaguchi K. 2009. Efficacy of colistin combination therapy in a mouse model of pneumonia caused by multidrug-resistant Pseudomonas aeruginosa. J Antimicrob Chemother 63:534–542. https://doi.org/10.1093/jac/dkn530.
54. Duff GW, Atkins E. 1982. The inhibitory effect of polymyxin B on endotoxin-induced endogenous pyrogen production. J Immunol Methods 52:333–340. https://doi.org/10.1016/0022-1759(82)90005-9.
55. Cockerill F, Patel J, Alder J, Bradford P, Dudley M, Eliopoulos G. 2013. Performance standards for antimicrobial susceptibility testing: 23rd informational supplement; M100-S23. Clinical and Laboratory Standards Institute, Wayne, PA.
56. Bivas-Benita M, Zwier R, Junginger HE, Borchard G. 2005. Non-invasive pulmonary aerosol delivery in mice by the endotracheal route. Eur J Pharm Biomed 61:214–218. https://doi.org/10.1016/j.ejpb.2005.04.009.
57. Cheah S-E, Bulitta JB, Li J, Nation RL. 2014. Development and validation of a liquid chromatography–mass spectrometry assay for polymyxin B in bacterial growth media. J Pharm Biomed Anal 92:177–182. https://doi.org/10.1016/j.jpba.2014.01.015.
58. Rennard S, Basset G, Lecossier D, O'Donnell KM, Pinkston P, Martin P, Crystal R. 1986. Estimation of volume of epithelial lining fluid recovered by lavage using urea as marker of dilution. J Appl Phys 60:532–538.
59. Bulitta JB, Landersdorfer CB. 2011. Performance and robustness of the Monte Carlo importance sampling algorithm using parallelized S-ADAPT for basic and complex mechanistic models. AAPS 13:212–226. https://doi.org/10.1208/s12248-011-9258-9.
60. Bergstrand M, Hooker AC, Wallin JE, Karlsson MO. 2011. Prediction-corrected visual predictive checks for diagnosing nonlinear mixed-effects models. AAPS 13:143–151. https://doi.org/10.1208/s12248-011-9255-z.
61. U.S. Food and Drug Administration. 1999. Guidance for industry. Population pharmacokinetics. U.S. Food and Drug Administration, Washington, DC.
62. Beal SL. 2001. Ways to fit a PK model with some data below the quantification limit. J Pharmacokinet Pharmacodyn 28:481–504. https://doi.org/10.1023/A:1012299115260.
63. Dudhani RV, Turnidge JD, Nation RL, Li J. 2010. fAUC/MIC is the most predictive pharmacokinetic/pharmacodynamic index of colistin against Acinetobacter baumannii in murine thigh and lung infection models. J Antimicrob Chemother 65:1984–1990. https://doi.org/10.1093/jac/dkq226.
64. Roberts KD, Azad MA, Wang J, Horne AS, Thompson PE, Nation RL, Velkov T, Li J. 2015. Antimicrobial activity and toxicity of the major lipopeptide components of polymyxin B and colistin: last-line antibiotics against multidrug-resistant gram-negative bacteria. ACS Infect Dis 1:568–575. https://doi.org/10.1021/acsinfecdis.5b00085.